DESY 15-034 2015

Impact of heavy-flavour production cross sections measured by the LHCb experiment on parton distribution functions at low x

PROSA Collaboration

O. Zenaiev[1], A. Geiser[1], K. Lipka[1], J. Blümlein[1], A. Cooper-Sarkar[2], M.-V. Garzelli[3], M. Guzzi[4], O. Kuprash[1], S.-O. Moch[3], P. Nadolsky[5], R. Placakyte[1], K. Rabbertz[6], I. Schienbein[7], P. Starovoitov[1]

[1]DESY Hamburg & Zeuthen, Germany, [2]University of Oxford, UK, [3]Universität Hamburg, Germany, [4]School of Physics and Astronomy, the University of Manchester, UK, [5]Southern Methodist University, Dallas, Texas, USA, [6]Karlsruher Institut für Technologie, Germany, [7]LPSC Grenoble, France.

Abstract

The impact of recent measurements of heavy-flavour production in deep inelastic ep scattering and in pp collisions on parton distribution functions is studied in a QCD analysis in the fixed-flavour number scheme at next-to-leading order. Differential cross sections of charm- and beauty-hadron production measured by LHCb are used together with inclusive and heavy-flavour production cross sections in deep inelastic scattering at HERA. The heavy-flavour data of the LHCb experiment impose additional constraints on the gluon and the sea-quark distributions at low partonic fractions x of the proton momentum, down to $x \sim 5 \times 10^{-6}$. This kinematic range is currently not covered by other experimental data in perturbative QCD fits.

1 Introduction

Understanding the nucleon structure is one of the fundamental tasks of modern particle physics. In quantum chromodynamics (QCD), the structure of the nucleon is described by parton distribution functions (PDFs), which, in collinear factorisation, represent probability densities to find a parton of longitudinal fraction x of the nucleon momentum at a factorisation scale μ_f. The scale evolution of the PDFs is uniquely predicted by the renormalisation group equations for factorisation [1, 2]. The x-dependence cannot be derived from first principles and must be constrained by experimental measurements. The precision of the PDFs is of key importance for interpreting the measurements in hadronic collisions. In particular, the uncertainty of the proton PDFs must be significantly reduced in order to improve the accuracy of theory predictions for Standard Model (SM) processes at the LHC.

Deep inelastic lepton-proton scattering (DIS) experiments cover a broad range in x and μ_f. In the perturbative regime, a wide x-range of $10^{-4} < x \lesssim 10^{-1}$ is probed by the data of the H1 and ZEUS experiments at the HERA collider [3]. These measurements impose the tightest constraints on the existing PDFs. However, additional measurements are necessary for a better flavour separation and to constrain the kinematic ranges of very small and very high x, where the gluon distribution is poorly known. A better constraint on the high-x gluon is needed for an accurate description of the SM backgrounds in searches for new particle production at high masses or momenta. Significant reduction of the uncertainty of the low-x gluon distribution is important for studies of parton dynamics, non-linear and saturation effects. Furthermore, precision of the gluon distribution at low x has implications in physics of atmospheric showers, being crucial for cross-section predictions of high-energy neutrino DIS interaction [4] and for calculations of prompt lepton fluxes in the atmosphere [5].

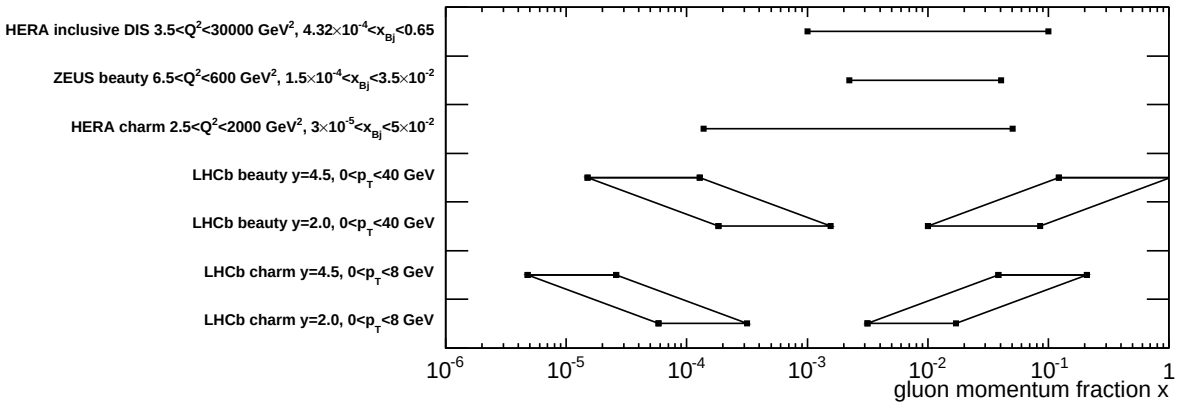

Figure 1: Kinematic range in x for the gluon density covered by measurements at HERA and LHCb. For the HERA inclusive DIS data, the x range is indicated, where the gluon PDF uncertainties are less than 10% at $\mu_f^2 = 10$ GeV^2. For the LHCb data, the upper (lower) edge of the box refers to the indicated upper (lower) end of the rapidity, y, range of the heavy-hadron production.

Heavy-flavour measurements of the LHCb Collaboration [6, 7] at the LHC probe the very forward range of the heavy-hadron rapidity y and are sensitive to the gluon PDF at low x, as schematically shown in Fig. 1. For this illustration, in the calculation of the kinematics of heavy-quark production at HERA, the leading order (LO) relation is used for the typical gluon x in boson-gluon fusion, $x = x_{Bj}(1 + \frac{4m_Q^2}{Q^2})$, where x_{Bj} denotes the Bjorken scaling variable, m_Q is the heavy-quark mass, and Q^2 is the virtuality of the exchanged electroweak boson. In the case of heavy-quark production at LHCb, the LO formula $x = e^{\pm y}\frac{\sqrt{p_T^2+m_Q^2}}{E_p}$, assuming $p_z = 0$ in the parton-parton rest frame, is applied. Here, p_T and p_z represent the transverse and longitudinal momenta of the heavy quark, respectively, and E_p is the proton beam energy.

Heavy-flavour production in proton-proton collisions at LHC is dominated by the gluon-gluon fusion process. Therefore the LHCb measurements of charm [6] and beauty [7] production in the forward region $2.0 < y < 4.5$ probe the gluon distribution at $5 \times 10^{-6} \lesssim x \lesssim 10^{-4}$, a region which is not accessible with HERA data. Note that the LHCb data are sensitive to the product of gluon densities in two non-overlapping low and medium-to-high x ranges, as illustrated in Fig. 1. Since the medium range is already well constrained by HERA data, which furthermore bridge the gap between the two LHCb ranges, the major impact of the LHCb heavy-flavour measurements is expected at $5 \times 10^{-6} \lesssim x \lesssim 10^{-4}$. The advantage of using heavy-flavour data is that the charm and beauty masses provide hard scales for the perturbative QCD expansion all the way down to their production threshold. To estimate the impact of the LHCb measurement of charm and beauty production on the gluon distribution at low x, these data are included in a QCD analysis together with the inclusive DIS [3] and heavy-flavour production [8, 9] cross sections measured at HERA.

2 Experimental data used in the QCD analysis

The main objective of the present QCD analysis is to demonstrate the constraining power of the measurements of heavy-flavour production in DIS and pp collisions for the determination of the PDFs of the proton. The measurements of charm and beauty production at HERA and LHCb, together with the combined HERA inclusive cross-section measurements, are used in a next-to-leading order (NLO) perturbative QCD (pQCD) analysis.

Neutral current (NC) and charged current (CC) inclusive DIS cross sections in ep scattering are directly sensitive to the valence and sea-quark distributions and probe the gluon distribution through scaling violations [1]. HERA measurements of the NC and CC cross sections in DIS at a centre-of-mass energy $\sqrt{s}$ = 320 GeV have been combined taking into account systematic correlations [3]. This combined data set contains the complete information on inclusive DIS cross sections published by the H1 and ZEUS Collaborations based on data collected in the years 1994-2000, and has been used for the determination of the PDF set HERAPDF1.0 [3]. The kinematic range of the NC data is $6 \times 10^{-7} \leq x_{Bj} \leq 0.65$, $0.045 \leq Q^2 \leq 30000$ GeV^2. The CC cross sections span the kinematic range of $1.3 \times 10^{-2} \leq x_{Bj} \leq 0.40$ and $300 \leq Q^2 \leq 30000$ GeV^2. These combined NC $e^{\pm}p$ and CC $e^{\pm}p$ cross sections represent the basis for all PDF determinations.

In ep scattering, charm and beauty quarks are produced predominantly in the photon-gluon fusion process which provides a direct probe of the gluon distribution in the proton. Measurements of open-charm production cross sections in DIS at HERA from the H1 and ZEUS Collaborations have been combined [8]. Cross sections for charm production were obtained in the kinematic range

of $2.5 \leq Q^2 \leq 2000$ GeV^2 and $3 \times 10^{-5} \leq x_{Bj} \leq 5 \times 10^{-2}$. The combination method accounts for the correlations of the systematic uncertainties among the different data sets. These combined measurements were used to improve constraints on the gluon distribution and to determine the charm-quark mass [8]. The charm reduced cross sections determined as a function of Q^2 and x_{Bj} are used in the present analysis together with all provided details on the systematic correlations. In addition, cross sections for the production of b quarks in ep scattering, as measured by the ZEUS Collaboration [9] are used in the present analysis. These data correspond to an integrated luminosity of 354 pb^{-1} and cover the kinematic range of $5 < Q^2 < 1000$ GeV^2. The b- and c-quark content in the events with at least one jet have been extracted using the invariant mass of charged tracks associated with secondary vertices and lifetime information, and the b-quark mass has been measured [9]. In the present analysis, the b-quark production data are used mainly to improve constraints on the b-quark mass.

For additional constraints on the gluon distribution at low x the differential cross sections of charm and beauty production in pp collisions at $\sqrt{s} = 7$ TeV from the LHCb experiment are used for the first time. The measurement of charm production [6] is based on data corresponding to an integrated luminosity of 15 nb^{-1}. Charm production is identified through the full reconstruction of decays of the charmed hadrons[1] D^0, D^+, D^{*+}, D_s^+ and Λ_c^+. The cross sections are measured as a function of the transverse momentum, p_T, and rapidity, y, of the reconstructed hadrons. The LHCb data on B-meson production in pp collisions [7] correspond to an integrated luminosity of 0.36 fb^{-1}. The B^+, B^0 and B_s^0 mesons are reconstructed in exclusive decays mainly involving J/ψ final states. Correlations between the experimental systematic uncertainties are accounted for as described in the original publications. An uncorrelated systematic uncertainty is obtained for each distribution by subtracting the correlated uncertainties from the total ones. The 3.5% luminosity uncertainty is treated as correlated between the measurements of charm and beauty production. In the present analysis, the normalised cross sections, $\frac{\mathrm{d}\sigma}{\mathrm{d}y}/\frac{\mathrm{d}\sigma}{\mathrm{d}y_0}$, for charm and beauty production are calculated from the absolute measurements published by LHCb and are used in the QCD analysis, with $\frac{\mathrm{d}\sigma}{\mathrm{d}y_0}$ being the cross section in the center bin, $3 < y < 3.5$, of the measured rapidity range in each p_T bin. The uncorrelated experimental uncertainty on $\frac{\mathrm{d}\sigma}{\mathrm{d}y_0}$ is propagated as a correlated uncertainty to the respective complementary rapidity bins. The QCD analysis is performed by using both, absolute or normalised, representations of the LHCb measurements, alternatively.

3 Theoretical predictions for heavy-flavour production

In the QCD analysis, the experimental measurements are confronted with corresponding theoretical predictions. The theoretical predictions for charm and beauty production in both ep and pp collisions are obtained at NLO in the fixed-flavour number scheme (FFNS). This scheme and its applicability to HERA measurements is discussed in detail in Ref. [8] and references therein. Predictions for HERA data are obtained by following the approach of the ABM group at NLO using its implementation in OPENQCDRAD [10] in the framework of HERAFitter [11]. The number of active flavours is set to $N_f = 3$, and the renormalisation and factorisation scales (pQCD scales) for heavy flavour production are chosen as $\mu_r = \mu_f = \sqrt{Q^2 + 4m_Q^2}$, where m_Q denotes the pole mass

[1] Charge conjugation is always implied for charm and beauty hadrons.

of c or b quarks[2]. For the light-flavour contributions to the inclusive DIS cross sections, the pQCD scales are set to $\mu_r = \mu_f = Q$.

Theoretical predictions for heavy-quark production in pp collisions are obtained using the massive NLO calculations [12–14] in the FFNS, also available as part of the Mangano-Nason-Ridolfi (MNR) calculations [15]. The pQCD scales are chosen as $\mu_{r,f} = A^{c,b}_{r,f}\mu_0$, with $\mu_0 = \sqrt{p_T^2 + m_Q^2}$ and $A^{c,b}_{r,f}$ being coefficients for c and b quarks, which are discussed in the following. These predictions were used successfully for beauty production in $p\bar{p}$ collisions at the $Sp\bar{p}S$ [16] and the Tevatron[3] [17]. They are conceptually very similar to the Frixione-Mangano-Nason-Ridolfi (FMNR) predictions [21] employed for heavy-flavour photoproduction at HERA [22].

The cross-section predictions for heavy-flavoured hadron production not only depend on the kinematics of the heavy-flavour production mechanism, but also on the fragmentation of the heavy quark into a particular final-state hadron. There is no final-state factorisation scale in the FFNS since collinear logarithms of the heavy-quark mass are included in fixed-order perturbation theory. The calculations in [12–14, 23] describe the production of an on-shell heavy quark. Near the kinematic threshold, the transition of the heavy quark into the observed heavy-flavoured hadron can be taken into account by multiplying the cross section with the appropriate branching fraction. This leads to an excellent description of B- and D-meson production measurements at the Tevatron and the LHC from $p_T = 0$ up to $p_T \sim 4m$ [24, 25]. The scope of these calculations can be extended by convoluting the heavy-quark production cross section with a suitable scale-independent fragmentation function describing the hadronisation of the heavy quark. The implementation of the convolution is not unique once the quark and hadron masses are taken into account, and leads to a potentially p_T-dependent modelling uncertainty which is, however, small compared to the scale-choice uncertainty at NLO. This fragmentation function is used on a purely phenomenological basis, since it does not strictly appear in the context of a factorisation theorem, and therefore it has to be extracted from data. It depends on the order of the perturbation series but is generally assumed to be otherwise universal. Its main effect is to lower the theoretical predictions at large p_T. Typical parametrisations used in the literature are those by Peterson et al. [26] depending on one parameter ε and by Kartvelishvili et al. [27] depending on one parameter α_K.

For the HERA measurements, the fragmentation functions and their uncertainties are considered and accounted for in the original publications [8, 9]. The measurements of LHCb are provided as hadron-production cross sections and the fragmentation functions have to be applied explicitly in order to use these data in the QCD analysis. In addition, fragmentation fractions describing the probability of a quark to fragment into a particular hadron have to be applied. The fragmentation fractions for c-flavoured hadrons are taken from [28] and for b-flavoured hadrons from [29].

So far, no fragmentation measurements were performed in pp collisions. Because of similarities of the c-quark production kinematics at HERA and LHCb, the Kartvelishvili fragmentation

[2]The pole mass is used for consistency with the pp predictions, since $\overline{\text{MS}}$ running mass predictions are not available for LHCb.

[3]Provided that fragmentation and other uncertainties are properly treated [18]. Note that the NLO+NLL (FONLL) [19] calculations used there, and also used by LHCb [6, 7], slightly reduce the cross sections at high transverse momenta with respect to the pure NLO calculation, while they are identical at low transverse momenta [19]. The Tevatron data are well described by FONLL [18]. This conclusion is also applicable to the NLO calculations [14] used here, since these were used as input for the NLO part of the FONLL calculations. The claim in [17] that the NLO predictions undershoot the data while FONLL describes them must thus be attributed to parametrisations beyond the perturbative part of the calculations, as illustrated, e.g., in Fig. 7 of [20].

function [27] with $\alpha_K = 4.4 \pm 1.7$, as obtained from corresponding HERA measurements [30, 31] extracted for the NLO FFNS scheme, is applied for predictions of the LHCb measurements of charm-hadron production. The fragmentation is performed in the laboratory frame by rescaling the quark three-momentum with the energy of the produced hadron being calculated using the hadron mass. This procedure is used for D^+ and D_s^+ mesons, and for Λ_c^+ baryons. For D^0- and D^+-meson production, the contribution from D^{*+} and D^{*0} mesons is treated as described in [32]. For beauty production, the value $\alpha_K = 11 \pm 4$ is used for all b-flavored hadrons, corresponding to measurements at LEP [33].

The fragmentation-fraction uncertainties are assigned to the measurements and are treated as correlated, while the uncertainties arising from the variations of assumptions on the fragmentation functions are treated in the form of variations of the theory predictions in the QCD fit.

4 Details of the QCD analysis

The open source QCD fit framework for PDF determination HERAFitter [11], version 1.0.0, is used. The partons are evolved by using the QCDNUM program [34]. The analysis-specific modifications to HERAFitter address the heavy-flavour treatment as follows. The massive fixed-flavour number scheme [35] with the number of flavours $N_f = 3$ is used for the treatment of heavy-flavour contributions. The calculation of one-particle inclusive heavy-quark production cross sections in hadron collisions at NLO according to [14] is implemented by using original routines from the MNR code [36]. The results agree with those obtained with the original MNR code at a level of accuracy below 1%.

The 3-flavour strong coupling constant in the NLO $\overline{\rm MS}$ scheme is set to $\alpha_S(m_Z)^{N_f=3} = 0.1059 \pm 0.0005$, which corresponds to the world average value of $\alpha_S(m_Z)^{N_f=5} = 0.1185 \pm 0.0006$, using two-loop evolution equations [34].

The Q^2 range of the inclusive HERA data is restricted to $Q^2 > Q^2_{min} = 3.5$ GeV^2. The procedure for the determination of the PDFs follows the approach used in the HERAPDF1.0 QCD fit [3]. The following independent combinations of parton distributions are chosen in the fit procedure at the initial scale of the QCD evolution $Q_0^2 = 1.4$ GeV^2: the valence-quark distributions $xu_{\rm v}(x)$, $xd_{\rm v}(x)$, the gluon distribution $xg(x)$ and the u-type and d-type anti-quark distributions (which are identical to the sea-quark distributions), $x\overline{\rm U}(x)$, $x\overline{\rm D}(x)$, where $x\overline{\rm U}(x) = x\overline{u}(x)$ and $x\overline{\rm D}(x) = x\overline{d}(x) + x\overline{s}(x)$. At the scale Q_0, the parton distributions are represented by

$$
\begin{aligned}
xu_{\rm v}(x) &= A_{u_{\rm v}}\, x^{B_{u_{\rm v}}}\, (1-x)^{C_{u_{\rm v}}}\, (1 + E_{u_{\rm v}} x^2), && (1)\\
xd_{\rm v}(x) &= A_{d_{\rm v}}\, x^{B_{d_{\rm v}}}\, (1-x)^{C_{d_{\rm v}}}, && (2)\\
x\overline{\rm U}(x) &= A_{\overline{\rm U}}\, x^{B_{\overline{\rm U}}}\, (1-x)^{C_{\overline{\rm U}}}, && (3)\\
x\overline{\rm D}(x) &= A_{\overline{\rm D}}\, x^{B_{\overline{\rm D}}}\, (1-x)^{C_{\overline{\rm D}}}, && (4)\\
xg(x) &= A_g\, x^{B_g}\, (1-x)^{C_g} - A'_g\, x^{B'_g}\, (1-x)^{C'_g}. && (5)
\end{aligned}
$$

The normalisation parameters $A_{u_{\rm v}}$, $A_{d_{\rm v}}$, A_g are determined by the QCD sum rules, the B parameters are responsible for the small-x behaviour of the PDFs, and the parameters C describe the shape of the distribution as $x \to 1$. A flexible form for the gluon distribution is adopted with the choice of $C'_g = 25$ motivated by the approach of the MSTW group [37, 38]. The s-quark distribution is defined through x-independent strangeness fraction, f_s, of the d-type sea, $x\overline{s} = f_s x\overline{D}$ at Q_0^2, where

$f_s = 0.31^{+0.19}_{-0.08}$ as in the analysis of [38], including the recent complementary measurement [39]. Additional constraints $B_{\overline{\mathrm{U}}} = B_{\overline{\mathrm{D}}}$ and $A_{\overline{\mathrm{U}}} = A_{\overline{\mathrm{D}}}(1 - f_s)$ are imposed, with $x\bar{u} \to x\bar{d}$ as $x \to 0$. The analysis is performed by fitting the remaining 13 free parameters in Eqs. (1–5).

The PDF parameters are determined in HERAFitter by minimisation of a χ^2-function taking into account correlated and uncorrelated uncertainties [40] of the measurements. Systematic uncertainties are assumed to be proportional to the central prediction values, whereas statistical uncertainties scale with the square root of the predictions. Correlated uncertainties are treated using nuisance parameter representation [40]. To minimise biases arising from the likelihood transition to χ^2 when the scaling of the errors is applied, a logarithmic correction is added to the χ^2-function [41].

The heavy-quark masses are left free in the fit. They are well constrained by the measurements of charm and beauty production in DIS and the fitted values (see Table 2 in the Appendix A) are consistent with the ones obtained in the corresponding HERA analyses [8, 9] within the intrinsic theoretical systematic uncertainty of the pole mass definition [42].

The QCD analysis is performed twice using either absolute or normalised differential cross sections of heavy-flavour production from LHCb measurements, as defined in Section 2. The implementation of the theory calculations [43] as described in Section 3 allows the pQCD scales, i.e. the parameters $A^{c,b}_{r,f}$, and the values for the pole mass of the heavy quarks to be changed at each fit iteration.

In the QCD analysis using the normalised LHCb measurements, the pQCD scales are fixed to $A_r = A_f = 1$ for the central result. The scale dependence is studied by varying the pQCD scales independently such that $0.5 \leq A_r, A_f \leq 2$. A^c and A^b are always varied simultaneously. The resulting scale dependence is small, since it is largely absorbed by the normalisation, as illustrated in Appendix A.

In the variant of the fit using the absolute LHCb cross sections, the scale dependence of the predicted cross section is the dominant theoretical uncertainty. The same scale choice and variation procedure, as applied for the variant of the fit using the normalised LHCb measurements, leads to unacceptably high χ^2 values of the respective fits [43]. Therefore, the four scales technically are treated as independent fully correlated systematic uncertainties for the central result. Since the pQCD scales are not physical parameters, the related uncertainties are not obtained from the fit. Instead, the effect of the scale choice on the other fitted parameters is evaluated by an independent variation of A_f in the range $0.5 < A^c_f = A^b_f < 2$ with A^c_r and A^b_r as free parameters, or A_r in the range $0.25 < A^c_r = A^b_r < 1$ with A^c_f and A^b_f being free parameters. For the variation $A^c_f = A^b_f = 0.5$, a cut $p_T > 2$ GeV is applied for the charm LHCb data to ensure that the factorisation scale is above 1 GeV^2, since this is technically required in the QCDNUM. This procedure ensures an acceptable fit quality for all variations [43], as required for a meaningful extraction of the other uncertainties. Because of the unconventional scale treatment the fit using absolute cross sections is considered to be a cross check.

5 PDF uncertainties

The PDF uncertainties are estimated following the approach of HERAPDF1.0 [3] in which experimental, model, and parametrisation uncertainties are taken into account. Experimental uncertainties are evaluated using the Hessian method [40]. A tolerance criterion of $\Delta\chi^2 = 1$ is adopted for

defining the fit uncertainties that originate from the experimental uncertainties of the measurements included in the analysis.

Model uncertainties arise from the variations in the values assumed for $Q^2_{\rm min}$ imposed on the HERA data, which is varied in the interval $2.5 \leq Q^2_{\rm min} < 5.0$ GeV^2; the fraction of strange quarks, varied in the range $0.23 < f_s < 0.50$ and the value of the strong coupling, varied in the range $0.1054 < \alpha_S(m_Z)^{N_F=3} < 0.1064$. The pQCD scales for heavy-quark production in DIS are varied simultaneously by a factor of 2 up and down for both, charm and beauty. For the fits with the LHCb data, the model uncertainties include theoretical uncertainties for the cross section predictions for heavy-flavoured hadron production, arising from variation of the pQCD scales and of the fragmentation parameters, as described in Section 3. Uncertainties, arising from these model variations are referred to as MNR uncertainties in the following.

The parametrisation uncertainty is estimated similarly to the HERAPDF1.0 procedure: for all parton densities, additional parameters are added one by one in the functional form of the parametrisations in Eqs. (1–5), in a similar way as described in [3, 8, 9]. Furthermore, the starting scale is varied to $Q^2_0 = 1.9$ GeV^2. The parametrisation uncertainty is constructed as an envelope built from the maximal differences between the PDFs resulting from all the parametrisation variations and the central fit at each x value. The total PDF uncertainty is obtained by adding experimental, model and parametrisation uncertainties in quadrature.

6 Results

In Fig. 2, the absolute cross sections for D^0- and B^+-meson production in pp collisions are shown for one representative rapidity bin and are compared to the theory predictions as used in the QCD analysis. A significant scale dependence is observed. The normalised cross sections for a representative p_T bin of the same data set are compared to the respective theory predictions in Fig. 3. The advantage of using the normalised cross section is a significant reduction of the scale dependence of the theoretical prediction, retaining the sensitivity of the cross sections to the gluon distribution. The reduction of the uncertainty due to scale variation is related to the fact that the scale choice affects mostly the normalisation but only to some extent the shape of heavy-quark production kinematics, as demonstrated in Fig. 6, 7 in the Appendix A.

The fit quality, represented by the total and partial values of χ^2 divided by the number of degrees of freedom, $n_{\rm dof}$, for both variants of the QCD analysis is presented in Table 1. When the normalised LHCb measurements are used in the QCD analysis, $n_{\rm dof}$ is appropriately reduced for the respective data sets. The fitted parameters are presented in Table 2 in the Appendix A.

The resulting gluon, valence-quark and sea-quark distributions with their total uncertainties are presented at $\mu_f^2 = 10$ GeV^2 in Fig. 4 and compared to the result of the fit, based on solely HERA measurements of inclusive and heavy-flavour DIS. The uncertainties on the gluon and sea-quark distributions at low x are significantly reduced in both cases, using LHCb absolute or normalised heavy-quark production cross sections. In case of the variant of the fit based on normalised LHCb cross sections, the uncertainties are reduced by more than a factor of three at $x \sim 5 \times 10^{-6}$, which is the edge of the sensitivity of the included measurements (Fig. 1). Consistent results are obtained in the fit using the absolute cross sections, which is considered an important cross check of the self-consistency of the NLO theory description.

The individual contributions of the experimental, model and parametrisation uncertainties for

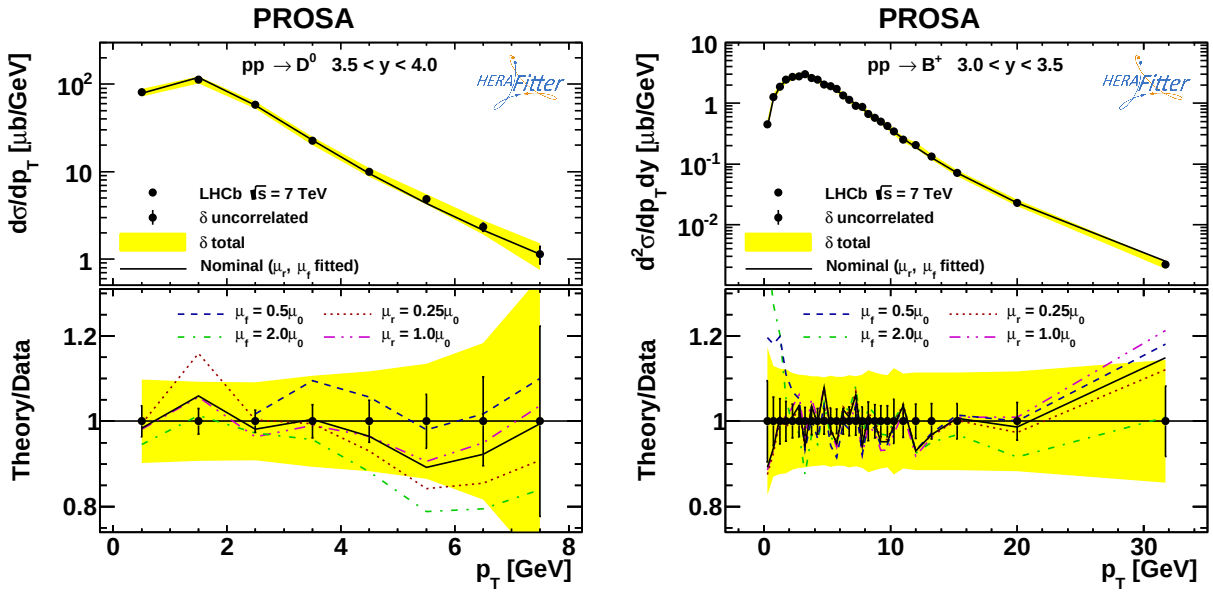

Figure 2: Data to theory comparison for a representative subset of the LHCb absolute cross sections for production of D^0 mesons for $3.5 < y < 4.0$ (left) and of B^+ mesons for $3.0 < y < 3.5$ (right). In the bottom panels the ratios theory/data for the nominal variant of the fit and the scale variations are shown. For demonstration purpose, correlated shifts for data points obtained in the fit using nuisance parameters are applied to theoretical predictions. Uncorrelated uncertainties for data points are shown as they are rescaled in the fit, while total uncertainties are shown as not rescaled.

both cases of using the LHCb measurements are shown in Fig. 5 and compared to the result of the fit using only HERA data. The gluon distribution at low x is constrained by the HERA measurements mostly via the sum rules and this results in large parametrisation uncertainties. Once the LHCb measurements are included in the QCD analysis, the gluon distribution is directly probed and the parametrisation dependence of the PDF is significantly reduced.

The main differences in the PDF uncertainties between the fits using the absolute and normalised LHCb measurements are caused by the MNR uncertainties. The variation of the pQCD scales in the prediction of the absolute cross section of heavy-flavour production in pp collisions leads to significant changes in the normalisation of the cross section and represents the dominant uncertainty on the PDFs. The variations of the assumption on fragmentation parameters [43] result in a smaller uncertainty, as compared to that due to the scale variations.

In the case of the PDF fit using the normalised LHCb cross sections, the MNR uncertainty is strongly reduced, since variations of pQCD scales and of the fragmentation parameters do not significantly affect the shape of the y distributions for heavy-flavour production. Therefore this is considered to be the primary result of this paper, while the consistency between the absolute and normalised variants is considered to be an important cross check.

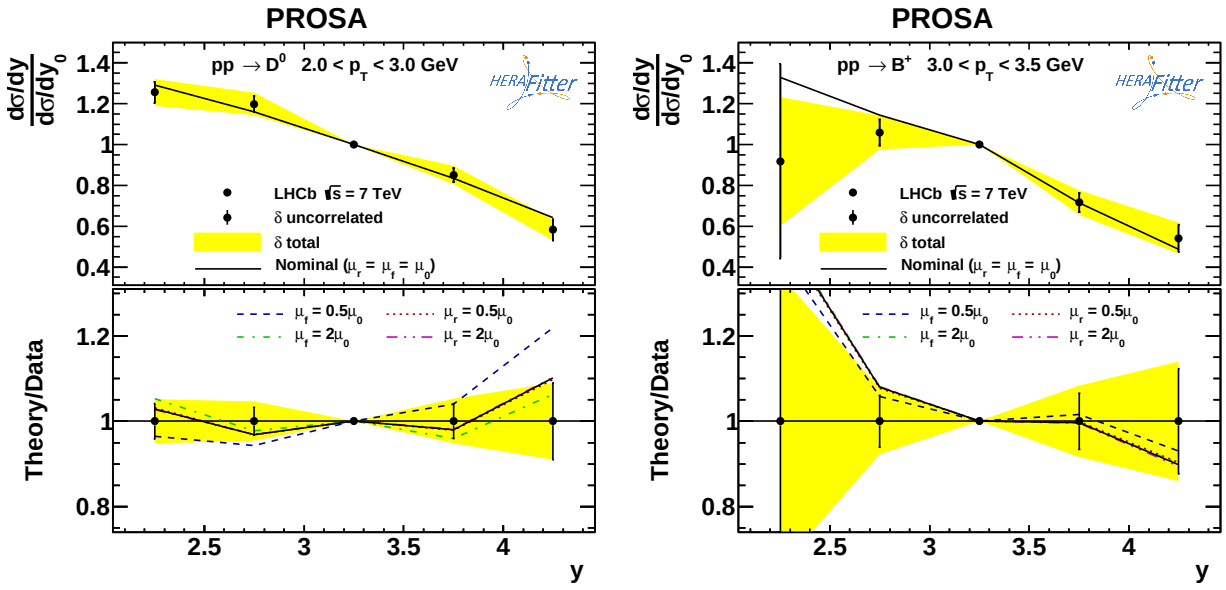

Figure 3: Data to theory comparison for a representative subset of the LHCb normalised cross sections for production of D^0 mesons for $2.0 < p_T < 3.0$ GeV (left) and of B^+ mesons for $3.0 < p_T < 3.5$ GeV (right). The central rapidity bins are fixed to 1 by the definition of the normalised cross sections. In the bottom panels the ratios theory/data for the nominal variant of the fit and the scale variations are shown. For demonstration purpose, correlated shifts for data points obtained in the fit using nuisance parameters are applied to theoretical predictions. Uncorrelated uncertainties for data points are shown as they are rescaled in the fit, while total uncertainties are shown as not rescaled.

7 Conclusions

The sensitivity of heavy-flavour production in pp collisions to the low-x gluon distribution was studied in a comprehensive QCD analysis at NLO. The measurements of c- and b-hadron production cross sections at the LHCb experiment are included into a PDF fit together with inclusive and heavy-flavour production measurements in DIS at HERA. Since the bulk of the heavy-flavour data is close to the kinematic threshold, the fixed-flavour number scheme at next-to-leading order is used for the predictions of heavy-flavour production in ep and pp collisions. A significant reduction of the parametrisation uncertainty of the gluon distribution at very low x is observed, as compared to the result of the PDF fit using only HERA DIS data.

Two ways of using the LHCb measurements in the fit are studied. Although the absolute differential cross-section measurements contain more information, the resulting PDFs suffer from large theoretical uncertainty due to uncalculated higher-order corrections, estimated by the variation of the pQCD scales. By using only the rapidity shape information in the normalised cross sections for the final result, this uncertainty is significantly reduced for the PDF extraction.

The present analysis has illustrated the high potential of the LHCb measurements to constrain the gluon distribution at low x, and global PDF fits clearly can profit from the inclusion of such data. Precise measurements of normalised cross sections of heavy-flavour production in the forward kinematic range of the LHC therefore have a great potential to further improve the constraints on

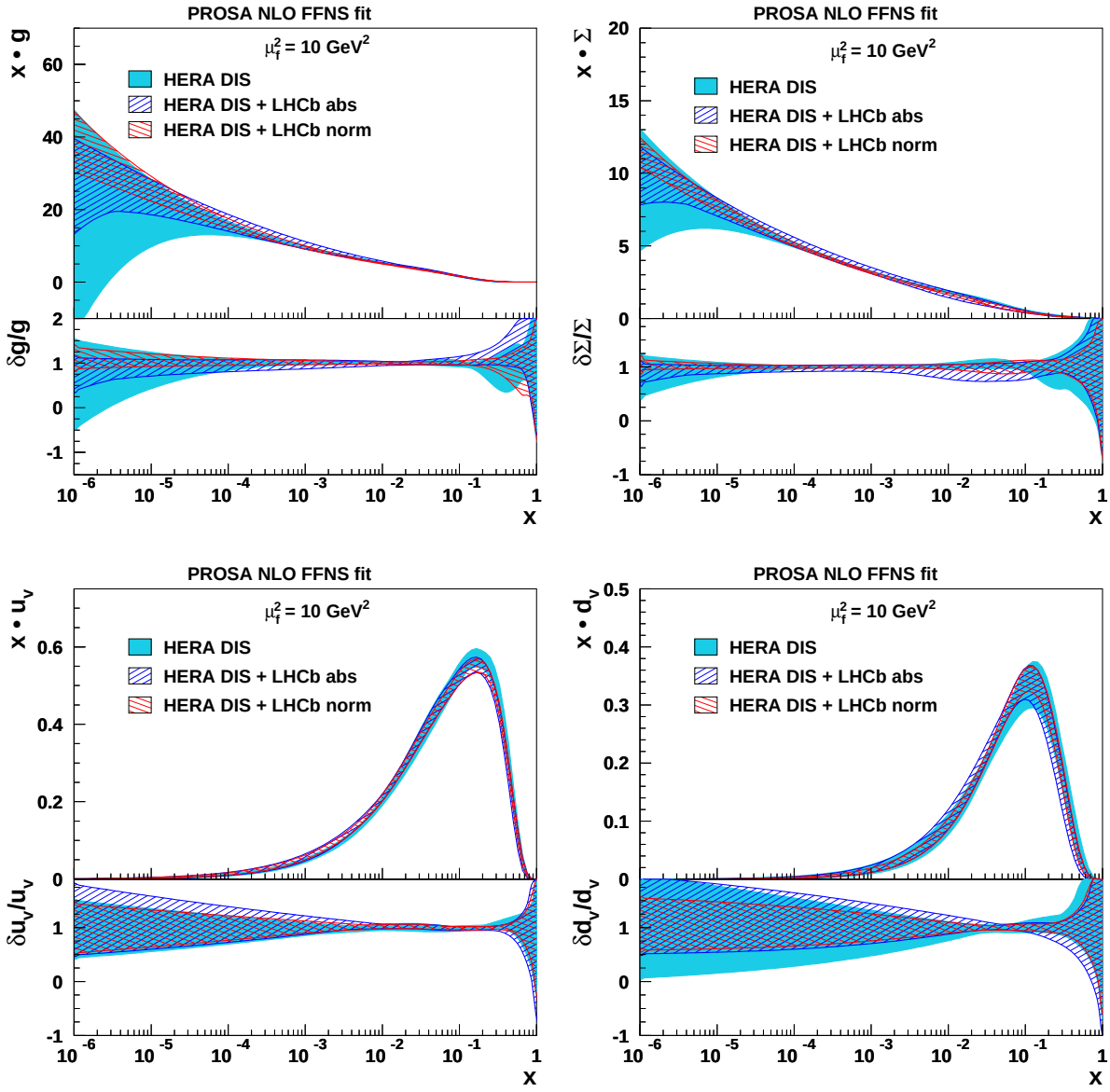

Figure 4: The gluon (top left), the sea-quark (top right), the u-valence quark (bottom left) and the d-valence quark (bottom right) distributions represented at $\mu_f^2 = 10$ GeV^2, as obtained in the QCD analysis of the HERA only data (light shaded band) and HERA and LHCb measurements and their relevant uncertainties. The sea-quark distribution is defined as $\Sigma = 2 \cdot (\bar{u} + \bar{d} + \bar{s})$. The results of the fit using absolute or normalised LHCb measurements are shown by different hatches. The widths of the bands represent the total uncertainties.

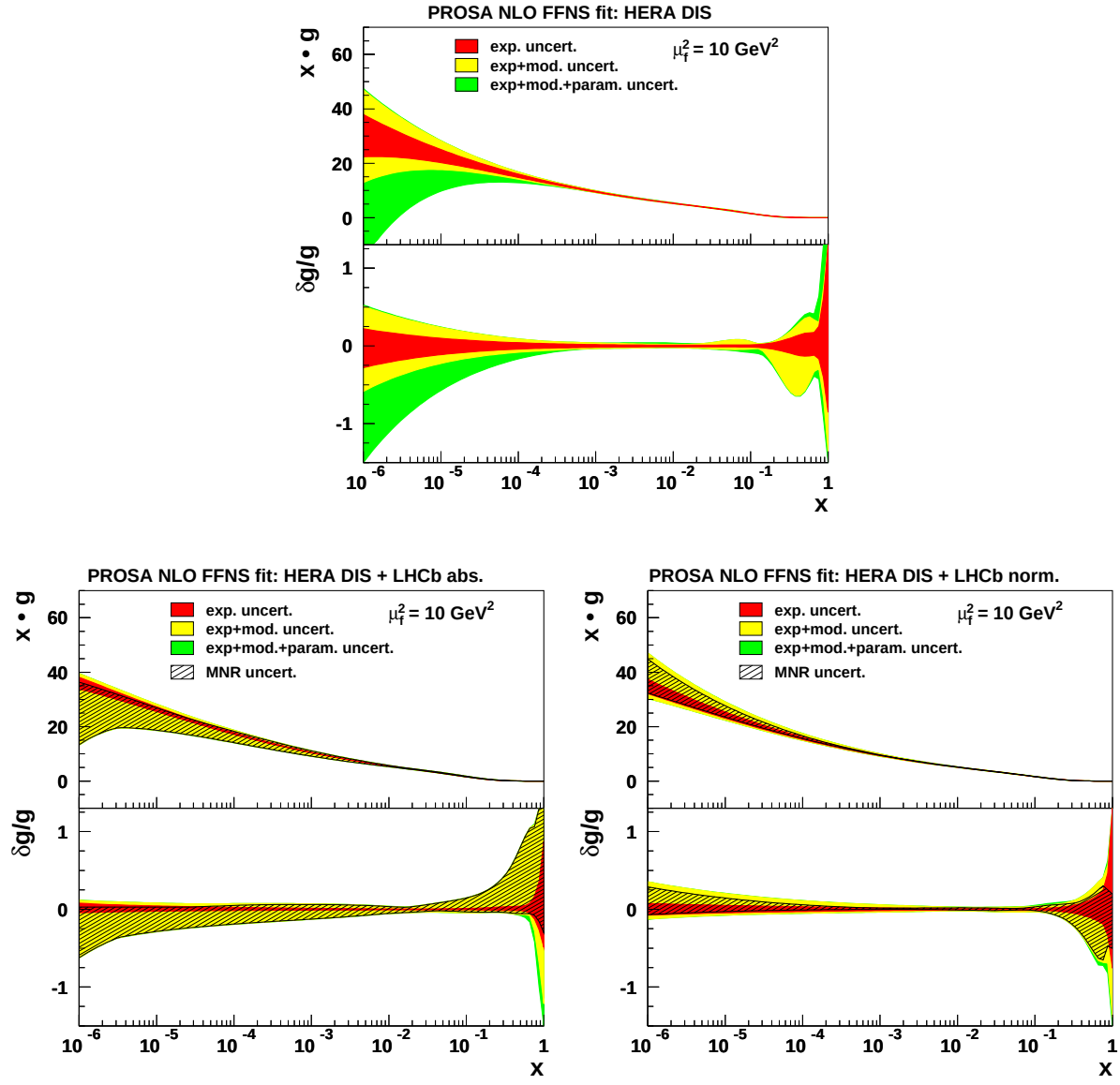

Figure 5: Individual contributions to the PDF uncertainties on the gluon distributions, obtained in QCD analyses using HERA-only (upper panel), HERA+LHCb absolute (lower panel left) and HERA+LHCb normalised (lower panel right) cross sections of heavy-flavour production.

Representation of the LHCb measurements	absolute	normalised
Global $\chi^2/n_{\rm dof}$	1073 / 1087	958 / 994
Global χ^2 p-value	0.61	0.79
χ^2-contribution from correlated uncertainties	73	49
χ^2-contribution from logarithmic correction	-129	48
Data set	partial $\chi^2/n_{\rm dof}$	
NC DIS HERA I combined e^-p	108 / 145	108 / 145
NC DIS HERA I combined e^+p	419 / 379	419 / 379
CC DIS HERA I combined e^-p	26 / 34	26 / 34
CC DIS HERA I combined e^+p	39 / 34	41 / 34
$c\bar{c}$ DIS HERA combined	78 / 52	47 / 52
$b\bar{b}$ DIS ZEUS Vertex	16 / 17	12 / 17
LHCb D^0	68 / 38	17 / 30
LHCb D^+	53 / 37	18 / 29
LHCb D^{*+}	50 / 31	19 / 22
LHCb D_s^+	24 / 28	11 / 20
LHCb Λ_c^+	5.3 / 6	4.9 / 3
LHCb B^+	99 / 135	81 / 108
LHCb B^0	66 / 95	35 / 76
LHCb B_s^0	78 / 75	23 / 60

Table 1: The global and partial χ^2 values for the data sets used in the analysis of HERA and LHCb measurements.

the PDFs.

In order to fully exploit the additional constraints from absolute LHC charm and beauty cross sections, a significant reduction of the theoretical uncertainties, e.g. through threshold resummation and/or (partial) NNLO calculations with codes suitable for a usage in QCD analyses, is desirable.

Acknowledgements

This work has been supported in part by the Helmholtz Association under contract numbers HGF-SO-072 and VH-HA-101. Supported in part by the EU-TMR Network Higgstools.

A Appendix

Parameter	absolute	normalised
B_g	-0.14 ± 0.07	-0.08 ± 0.10
C_g	6.83 ± 0.31	5.23 ± 0.34
A'_g	1.74 ± 0.22	1.29 ± 0.32
B'_g	-0.19 ± 0.04	-0.16 ± 0.05
B_{u_v}	0.668 ± 0.020	0.649 ± 0.021
C_{u_v}	4.99 ± 0.23	4.98 ± 0.23
E_{u_v}	12.2 ± 2.4	13.5 ± 2.7
B_{d_v}	0.93 ± 0.09	0.96 ± 0.09
C_{d_v}	5.50 ± 0.56	5.59 ± 0.55
$C_{\overline{\mathrm{U}}}$	1.63 ± 0.21	1.63 ± 0.24
$A_{\overline{\mathrm{D}}}$	0.173 ± 0.007	0.158 ± 0.007
$B_{\overline{\mathrm{D}}}$	-0.146 ± 0.006	-0.155 ± 0.007
$C_{\overline{\mathrm{D}}}$	10.4 ± 2.5	15.1 ± 4.2
m_c	1.709 ± 0.024	1.257 ± 0.014
m_b	4.67 ± 0.08	4.19 ± 0.13
A_f^c	0.659 ± 0.020	1.0
A_f^b	0.262 ± 0.007	1.0
A_r^c	0.444 ± 0.021	1.0
A_r^b	0.335 ± 0.024	1.0

Table 2: The fitted parameters for the NLO QCD analysis using HERA and LHCb measurements. The value of strong coupling $\alpha_S(m_Z)^{N_f=3} = 0.1059$ is used. The listed uncertainties correspond to those associated to the experimental measurements used in the fit. Uncertainties are not quoted for parameters that are fixed.

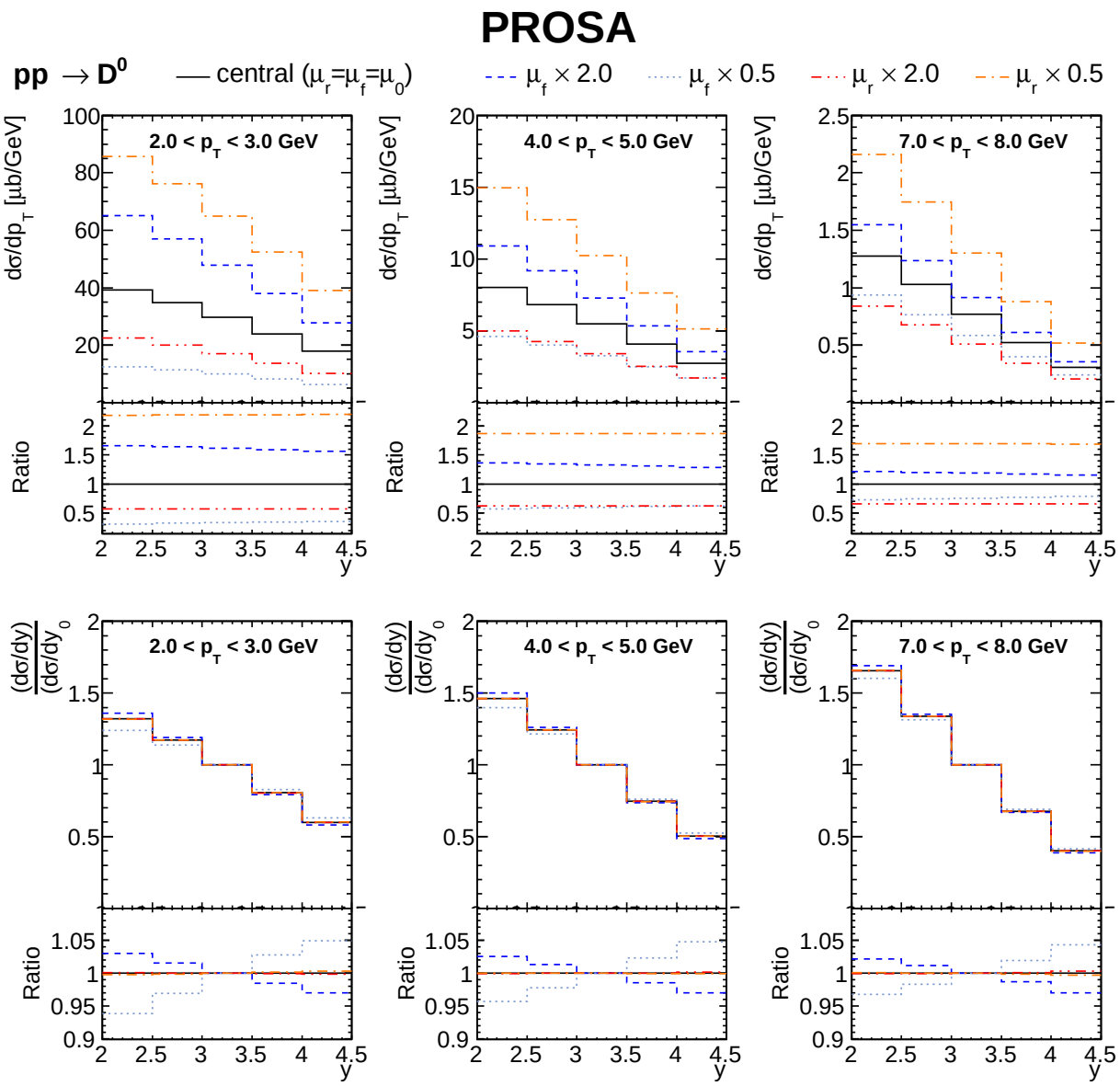

Figure 6: NLO QCD predictions for charm LHCb data with different scale choices for absolute (top) and normalised (bottom) cross sections. Lower inlets indicate the ratio of predictions to the central scale choice. The predictions are obtained by using the FFNS variant of MSTW 2008 PDFs [44] with $N_f = 3$; the charm mass is set to $m_c = 1.5$ GeV.

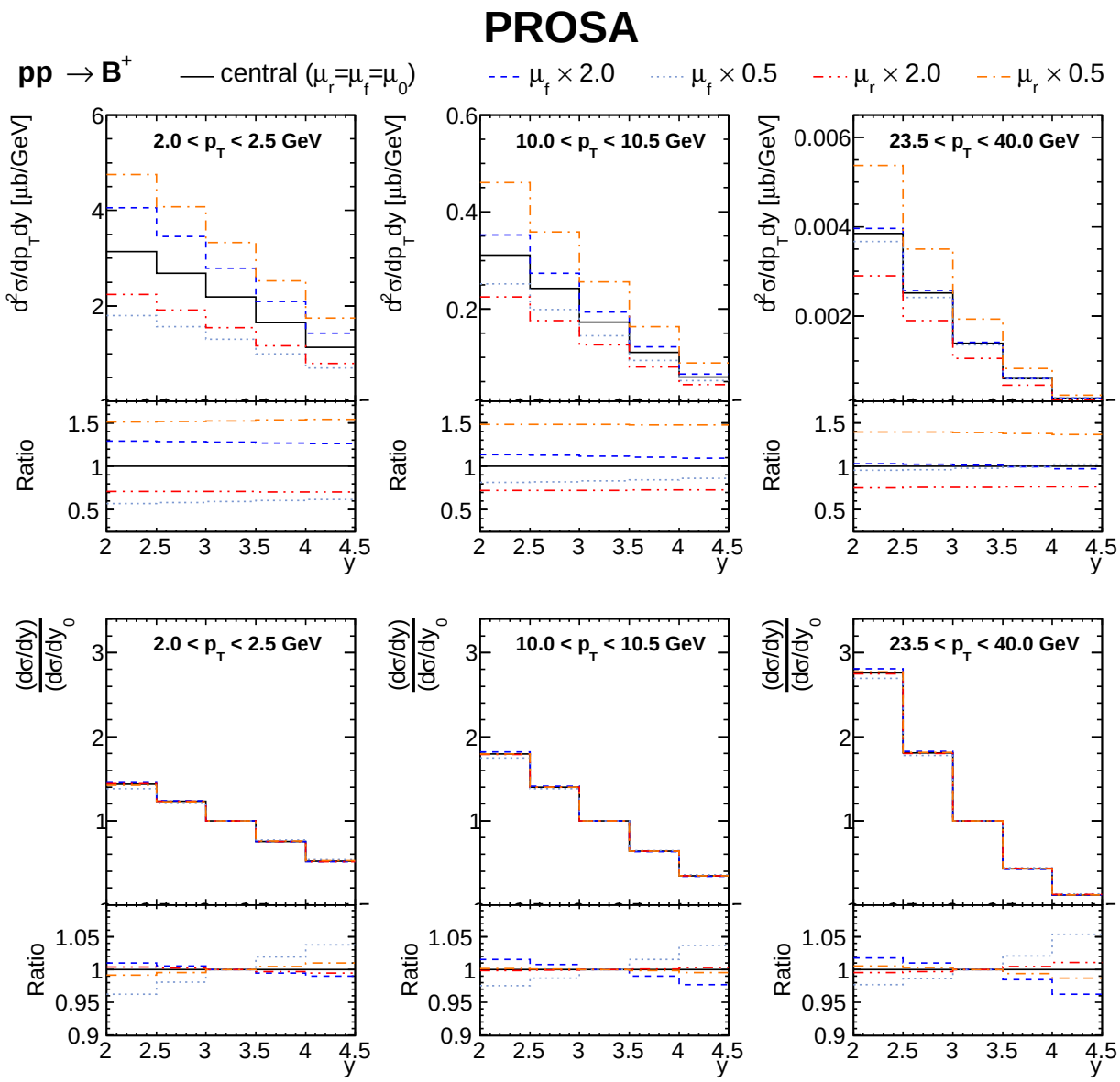

Figure 7: NLO QCD predictions for beauty LHCb data with different scale choices for absolute (top) and normalised (bottom) cross sections. Lower inlets indicate the ratio of predictions to the central scale choice. The predictions are obtained using the FFNS variant of MSTW 2008 PDFs [44] with $N_f = 3$; the beauty mass is set to $m_b = 4.5$ GeV.

References

[1] D. J. Gross and F. Wilczek, Phys. Rev. D8 (1973) 3633, doi: 10.1103/PhysRevD.8.3633;
D. J. Gross and F. Wilczek, Phys. Rev. D9 (1974) 980, doi: 10.1103/PhysRevD.9.980;
H. Georgi and H. D. Politzer, Phys. Rev. D9 (1974) 416, doi: 10.1103/PhysRevD.9.416.

[2] V. N. Gribov and L. N. Lipatov, Sov. J. Nucl. Phys. 15 (1972) 438;
G. Altarelli and G. Parisi, Nucl. Phys. B126 (1977) 298, doi:10.1016/0550-3213(77)90384-4;
G. Curci, W. Furmanski, and R. Petronzio, Nucl. Phys. B175 (1980) 27, doi:10.1016/0550-3213(80)90003-6;
W. Furmanski and R. Petronzio, Phys. Lett. B97 (1980) 437, doi:10.1016/0370-2693(80)90636-X;
S. Moch, J. A. M. Vermaseren, and A. Vogt, Nucl. Phys. B688 (2004) 101, doi:10.1016/j.nuclphysb.2004.03.030, [arXiv:hep-ph/0403192];
A. Vogt, S. Moch, and J. A. M. Vermaseren, Nucl. Phys. B691 (2004) 129, doi:10.1016/j.nuclphysb.2004.04.024, [arXiv:hep-ph/0404111].

[3] F. D. Aaron et al. [H1 and ZEUS Collaboration], JHEP01 (2010) 109, doi: 10.1007/JHEP01(2010)109, [arXiv:0911.0884].

[4] A. Cooper-Sarkar, P. Mertsch, S. Sarkar, JHEP08 (2011) 042, doi: 10.1007/JHEP08(2011)042, [arXiv:1106.3723].

[5] L. Pasquali, M. H. Reno, I. Sarcevic, Phys. Rev. D59 (1999) 034020, doi: 10.1103/PhysRevD.59.034020, [arXiv:hep-ph/9806428].

[6] R. Aaij et al. [LHCb Collaboration], Nucl. Phys. B871 (2013) 1, doi: 10.1016/j.nuclphysb.2013.02.010, [arXiv:1302.2864].

[7] R. Aaij et al. [LHCb Collaboration], JHEP08 (2013) 117, doi: 10.1007/JHEP08(2013)117, [arXiv:1306.3663].

[8] F. D. Aaron et al. [H1 and ZEUS Collaborations], Eur. Phys. J. C73 (2013) 2311, doi: 10.1140/epjc/s10052-013-2311-3, [arXiv:1211.1182].

[9] H. Abramowicz et al. [ZEUS Collaboration], JHEP09 (2014) 127, doi: 10.1007/JHEP09(2014)127, [arXiv:1405.6915].

[10] S. Alekhin, J. Blümlein, S. Moch, Phys. Rev. D86 (2012) 054009, doi: 10.1103/PhysRevD.86.054009, [arXiv:1202.2281];
I. Bierenbaum, J. Blümlein, S. Klein, Phys. Lett. B672 (2009) 401, doi: 10.1016/j.physletb.2009.01.057, [arXiv:0901.0669];
S. Alekhin, OPENQCDRAD-1.5. `http://www-zeuthen.desy.de/~alekhin/OPENQCDRAD`.

[11] S. Alekhin et al. [HERAFitter], [arXiv:1410.4412].

[12] P. Nason, S. Dawson, R. K. Ellis, Nucl. Phys. B303 (1988) 607, doi: 10.1016/0550-3213(88)90422-1.

[13] W. Beenakker, H. Kuijf, W. L. van Neerven, J. Smith, Phys. Rev. D40 (1989) 54, doi: 10.1103/PhysRevD.40.54.

[14] P. Nason, S. Dawson, R. K. Ellis, Nucl. Phys. B327 (1989) 49, doi: 10.1016/0550-3213(89)90286-1.

[15] M. L. Mangano, P. Nason and G. Ridolfi, Nucl. Phys. B373 (1992) 295, doi: 10.1016/0550-3213(92)90435-E.

[16] C. Albajar et al. [UA1 collaboration], Phys. Lett. B369 (1996) 46, doi: 10.1016/0370-2693(95)01539-6;
C. Albajar et al. [UA1 collaboration], Z. Phys. C61 (1994) 41, doi: 10.1007/BF01641885;
C. Albajar et al. [UA1 collaboration], Phys. Lett. B256 (1991) 121, doi: 10.1016/0370-2693(91)90228-I, Erratum-ibid. B262 (1991) 497.

[17] A. Abulencia et al. [CDF Collaboration], Phys. Rev. D75 (2007) 012010, doi: 10.1103/PhysRevD.75.012010, [arXiv:hep-ex/0612015].

[18] M. Cacciari and P. Nason, Phys. Rev. Lett. 89 (2002) 122003, doi: 10.1103/PhysRevLett.89.122003, [arXiv:hep-ph/0204025].

[19] M. Cacciari, M. Greco, and P. Nason, JHEP05 (1998) 007, doi: 10.1088/1126-6708/1998/05/007, [arXiv:hep-ph/9803400].

[20] B. A. Kniehl, G. Kramer, I. Schienbein and H. Spiesberger, Phys. Rev. D77 (2008) 014011, doi: 10.1103/PhysRevD.77.014011, [arXiv:0705.4392].

[21] S. Frixione et al., Phys. Lett. B348 (1995) 633, doi: 10.1016/0370-2693(95)00163-F.

S. Frixione, P. Nason, G. Ridolfi, Nucl. Phys. B454 (1995) 3, doi: 10.1016/0550-3213(95)00445-X, [arXiv:hep-ph/9506226].

[22] S. Aid et al. [H1 Collaboration], Nucl. Phys. B472 (1996) 32, doi: 10.1016/0550-3213(96)00275-1, [arXiv:hep-ex/9604005].

M. Derrick et al. [ZEUS Collaboration], Phys. Lett. B349 (1995) 225, doi: 10.1016/0370-2693(95)00253-H, [arXiv:hep-ex/9502002].

[23] W. Beenakker, W. L. van Neerven, R. Meng, G. A. Schuler and J. Smith, Nucl. Phys. B351 (1991) 507, doi: 10.1016/S0550-3213(05)80032-X.

[24] B. A. Kniehl, G. Kramer, I. Schienbein and H. Spiesberger, [arXiv:1502.01001].

[25] B. A. Kniehl, G. Kramer, I. Schienbein and H. Spiesberger, Eur. Phys. J. C72 (2012) 2082, doi: 10.1140/epjc/s10052-012-2082-2, [arXiv:1202.0439].

[26] C. Peterson, D. Schlatter, I. Schmitt, and P. Zerwas, Phys. Rev. D27 (1983) 105, doi: 10.1103/PhysRevD.27.105.

[27] V. Kartvelishvili, A. Likhoded and V. Petrov, Phys. Lett. B78 (1978) 615, doi: 10.1016/0370-2693(78)90653-6.

[28] E. Lohrmann, [arXiv:1112.3757].

[29] R. Aaij et al., JHEP08 (2013) 117, doi: 10.1007/JHEP08(2013)117, [arXiv:1306.3663].

[30] F. Aaron et al. [H1 Collaboration], Eur. Phys. J. C59 (2009) 589, doi: 10.1140/epjc/s10052-008-0792-2, [arXiv:0808.1003].

[31] S. Chekanov et al. [ZEUS Collaboration], JHEP04 (2009) 082, doi: 10.1088/1126-6708/2009/04/082, [arXiv:0901.1210].

[32] M. Cacciari and P. Nason, JHEP09 (2003) 006, doi: 10.1088/1126-6708/2003/09/006, [arXiv:hep-ph/0306212].

[33] P. Nason and C. Oleari, Nucl. Phys. B565 (2000) 245, doi: 10.1016/S0550-3213(99)00673-2, [arXiv:hep-ph/9903541].

[34] M. Botje, Comput. Phys. Commun. 182 (2011) 490, doi:10.1016/j.cpc.2010.10.020, [arXiv:1005.1481].

[35] E. Witten, Nucl. Phys. B104 (1976) 445, doi: 10.1016/0550-3213(76)90111-5;

E. Laenen, S. Riemersma, J. Smith and W. L. van Neerven, Nucl. Phys. B392 (1993) 162, doi: 10.1016/0550-3213(93)90201-Y;

I. Bierenbaum, J. Blümlein and S. Klein, Nucl. Phys. B820 (2009) 417, doi: 10.1016/j.nuclphysb.2009.06.005, [arXiv:0904.3563];

J. Blümlein, A. De Freitas and C. Schneider, [arXiv:1411.5669].

[36] The MNR code, `http://www.ge.infn.it/~ridolfi/hvqlibx.tgz`.

[37] R. S. Thorne, Phys. Rev. D73 (2006) 054019; doi: 10.1103/PhysRevD.73.054019, [arXiv:hep-ph/0601245].

[38] W. J. Stirling, R. S. Thorne and G. Watt, Eur. Phys. J C63 (2009) 189, doi: 10.1140/epjc/s10052-009-1072-5, [arXiv:0901.0002].

[39] G. Aad et al. [ATLAS Collaboration], Phys. Rev. Lett. 109 (2012) 012001, doi: 10.1103/PhysRevLett.109.012001, [arXiv:1203.4051].

[40] S. Alekhin, O. Behnke, P. Belov, S. Borroni, M. Botje, D. Britzger, S. Camarda, A. M. Cooper-Sarkar et al., [arXiv:1410.4412].

[41] F. D. Aaron et al. [H1 Collaboration], JHEP09 (2012) 061, doi: 10.1007/JHEP09(2012)061, [arXiv:1206.7007].

[42] I. I. Bigi, M. A. Shifman, N. Uraltsev, and A. Vainshtein, Phys. Rev. D50 (1994) 2234, doi: 10.1103/PhysRevD.50.2234, [arXiv:hep-ph/9402360];

M. Beneke and V. M. Braun, Nucl. Phys. B426 (1994) 301, doi: 10.1016/0550-3213(94)90314-X, [arXiv:hep-ph/9402364];

M. Beneke, Phys. Rept. 317 (1999) 1, doi: 10.1016/S0370-1573(98)00130-6, [arXiv:hep-ph/9807443].

[43] O. Zenaiev, "Charm Production and QCD Analysis at HERA and LHC", Ph. D. Thesis, Hamburg University, 2015.

[44] A. D. Martin, W. J. Stirling, R. S. Thorne and G. Watt, Eur. Phys. J. C70 (2010) 51, doi: 10.1140/epjc/s10052-010-1462-8, [arXiv:1007.2624].